Eur. Phys. J. D **35**, 513–520 (2005)
DOI: 10.1140/epjd/e2005-00169-6

THE EUROPEAN PHYSICAL JOURNAL D

Microsolvation of neutral dopants in small He clusters: relative locations of Li and Na atoms

C. Di Paola[1] and F.A. Gianturco[1,a]

Dept. of Chemistry and INFM, The University of Rome "La Sapienza", P.le A. Moro 5, 00185 Rome, Italy

Received 3 March 2005
Published online 21 June 2005 –

Abstract. Quantum Calculations of binding energies and spatial distributions are carried out using Diffusion Monte Carlo (DMC) methods for several bosonic helium clusters containing lithium and sodium atoms as neutral impurities. The global interaction forces have been constructed via sum-of-potentials models with accurate empirical potentials for the two-body (2B) forces, disregarding many-body (MB) effects on such weakly interacting systems. The results clearly show that both impurities can bind to the helium clusters but that they chiefly reside outside them and do not undergo microsolvation.

PACS. 34.30.+h Intramolecular energy transfer; intramolecular dynamics; dynamics of van der Waals molecules – 36.40.Mr Spectroscopy and geometrical structure of clusters – 36.40.Qv Stability and fragmentation of clusters

1 Introduction

In the last few years the study of helium clusters of a very broad range of sizes, and the behaviour of a correspondingly broad variety of atomic and molecular dopants contained by such varied droplets, has received considerable attention both by chemists and physicists because of their unique properties, determined in the main by quantum effects [1,2]. They are in fact known to be the only clusters that are liquid under all conditions of formation, due to the very large zero-point motions of the He adatoms which solidify only under pressure. It is therefore of interest to get to understand how the various properties of bulk liquid can emerge from those of the finite systems.

Thus, to study the spectral behaviour of atomic and molecular dopants attached to such droplets has provided in recent years a great deal of information by analysing the dopant spectra in the infrared and the visible regions [3–5]. Recent model theoretical studies of the microsolvated dopant molecules in either ^{4}He or ^{3}He droplets have also provided very useful indications on the molecular sources of spectral differences between bosonic/fermionic environments [6].

All the studies carried out so far have clearly shown that, due to the "softness" of the helium atoms, the liquid environments of the droplets remain very sensitive to their interaction with the dopant [1,2]. Thus, a positive ion surrounded by a shell of He atoms appears as being strongly compressed as a result of electrostriction effects [7,8], while a negative ion may be ejected by the droplet, thus residing largely on its outside [9]. As a further example, a free electron injected in helium droplets is capable of forming a large "bubble" of about 34 Å diameter [10]. It is therefore of importance to be able to relate as much as possible the experimentally found, or theoretically predicted behaviour of such microsolvation cases with the strength and features of the relevant intermolecular forces.

A case in point is provided by neutral alkali atoms attached to helium droplets, where they can play the role of the chromophoric dopants and their laser-induced fluorence (LIF) spectra can yield useful indicators on both structural and dynamical properties [11–13]. More recent calculations of the absorption spectra [14] for Li, Na and K as dopants have provided the positions, relative intensities and line widths of the absorption maxima as a function of cluster size and found them to be in moderate agreement with the existing experiments [15]. Those calculations were carried out using a pairwise, additive global potential model and disregarded any effect from possible MB contributions, as in the present study.

In the present work we thus intend to revisit the above findings in a slightly different way by analysing in more detail the quantum effects induced in He droplets: we shall examine the trend of binding energy values along a sequence of bosonic helium clusters doped by Li and Na atoms, respectively. We shall also analyse the similar trend of their quantum structures and suggest ways to represent pictorially the possible locations of the alkali dopant as the cluster grows, in order to show that our quantum treatment unequivocally confirms the dopant atoms to be placed on the outside of the cluster structures.

[a] e-mail: fa.gianturco@caspur.it

To our knowledge, the relative locations of such weakly bound atoms within He droplets has not been analysed in such detail before, although calculations with different methods have been done before as we shall discuss further in the following.

Next section briefly outlines our computational method of choice, the Quantum Diffusion Monte Carlo (DMC) method, and discusses the pairwise modelling of the global interactions, a simplification generally considered to be realistic enough for such weakly interacting species [6–8].

Section 3 reports and discusses our present results while Section 4 summarizes our conclusions.

2 Computing interaction and structures

2.1 The pairwise potential model

The largest contributions to the overall interaction potential within the cluster come from the isotropic forces between pairs of helium atoms, $V_{\mathrm{He-He}}(r_{ij})$, and the spherical potential between the alkali impurity and any of the cluster adatoms, $V_{\mathrm{Ak-He}}(r_{i\mathrm{Ak}})$. Further, MB contributions associated with cooperative interactions, or between all the adatoms among themselves, are disregarded in the present study because of the negligible effects that such additional forces are found to have for the very weakly interacting species of the clusters [6–8].

We therefore write the overall potential as

$$V_{tot}(\mathbf{R}_{\mathrm{Ak}}, \mathbf{R}_i) = \sum_{i<j}^{N} V_{\mathrm{He-He}}(\mathbf{R}_i) + \sum_{i=1}^{N} V_{\mathrm{Ak-He}}(\mathbf{R}_{i\mathrm{Ak}}) \quad (1)$$

where $\mathbf{R}_{ij} = |\mathbf{R}_i - \mathbf{R}_j|$ and $\mathbf{R}_{i\mathrm{Ak}} = |\mathbf{R}_i - \mathbf{R}_{\mathrm{Ak}}|$, where the subscript Ak labels the alkali dopant atom. The two pairwise potentials employed here have been already used by us in a recent analysis of the ground-state properties of the $^4He_2Li$ and $^4He_2Na$ systems [16]. They all originate from previous studies where the combined use of ab-initio results and empirical parameters was employed to obtain very accurate description of the pair potentials in question [17–19].

We report in Figure 1 a comparison of the chosen interactions for the Li–He, Na–He and He–He systems. We clearly see there that the interaction between the "solvent" atoms is markedly stronger than those between them and the alkali dopants: the minimum of the $V_{\mathrm{He-He}}$ well depth occurs at closer distances (∼3 Å) than those of the $V_{\mathrm{Ak-He}}$ potentials (∼6 Å) and it exhibits a deeper well (∼8 cm^{-1}) in comparison with that of the other two potentials (∼2 cm^{-1}). As as consequence of it, the onset of the repulsive wall of the $V_{\mathrm{He-He}}$ interaction occurs at shorter distances and appears to be less "soft" than the interactions between helium and the alkali dopants. In an earlier analysis of the dimer and trimer species [16], we had already shown that the use of the above interactions for the calculation of the ground state binding energies yielded results which were in good accord with those from earlier studies: we have therefore employed the same set of potentials for the present analysis.

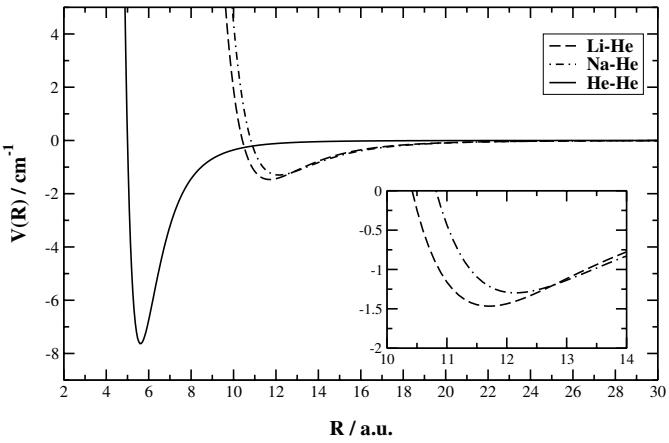

Fig. 1. Comparison of the empirical pairwise potentials employed in the present work. The He–He interaction is from reference [18] while the He–Ak potentials are from reference [19].

2.2 The quantum DMC method

The DMC method has been extensively discussed before (see [20–22] and references therein). We therefore refer the reader to that literature while this section merely summarizes the main features of the method. The key idea of the DMC method is the isomorphism between the solution of the time-dependent Schrödinger equation and that of a reactive-diffusion equation with anisotropic coefficients [20]. The Schrödinger equation for an N-dimensional system can be written as

$$\begin{aligned} i\hbar\frac{\partial\Phi(\mathbf{R},t)}{\partial t} &= \mathcal{H}\Phi(\mathbf{R},t) \\ &= -\sum_{j}^{N} D_j \nabla_j^2 \Phi(\mathbf{R},t) \\ &\quad + [V(\mathbf{R}) - E_{ref}]\,\Phi(\mathbf{R},t), \end{aligned} \quad (2)$$

where $\mathbf{R}$ describes a vector in the N-dimensional space and $D_j = \hbar^2/2m_j$. E_{ref} is a constant which defines the zero of the absolute energy scale and $V(\mathbf{R})$ is the potential function. After introducing the imaginary time $\tau = it$, one obtains the diffusion equation

$$\begin{aligned} \frac{\partial\Phi(\mathbf{R},\tau)}{\partial\tau} &= \sum_{j}^{N} D_j \nabla_j^2 \Phi(\mathbf{R},\tau) \\ &\quad - [V(\mathbf{R}) - E_{ref}]\,\Phi(\mathbf{R},\tau). \end{aligned} \quad (3)$$

In order to improve the efficiency of the method, and to increase its accuracy, one usually selects a guiding function Ψ_T which approximates the true solution of equation (2). The introduction of this function leads to the following diffusion-like equation for the product function

$f(\mathbf{R},\tau) = \Psi_T(\mathbf{R})\Phi(\mathbf{R},\tau)$:

$$\frac{\partial f(\mathbf{R},\tau)}{\partial \tau} = \Big[\sum_j \left(D_j\nabla_j^2 - D_j\nabla_j\cdot\mathbf{F}_j - D_j\mathbf{F}_j\cdot\nabla_j\right) - E_L(\mathbf{R}) + E_R\Big] f(\mathbf{R},\tau), \quad (4)$$

where $E_L(\mathbf{R}) = \Psi_T(\mathbf{R})^{-1}\mathcal{H}\Psi_T(\mathbf{R})$ is the local energy and the quantum force $\mathbf{F}_j(\mathbf{R}) = 2\nabla \ln \Psi_T(\mathbf{R})$. As long as this trial function is a reasonable approximation to the true ground state, the asymptotic solutions of equation (4) yield a mixed distribution function, which is now independent of τ

$$f_0(\mathbf{R}) = \Psi_T(\mathbf{R})\Phi_0(\mathbf{R}), \quad (5)$$

where $\Phi_0(\mathbf{R})$ is the true ground state wave function. The exact ground state energy is thus obtained as the average of the local energy $E_L(\mathbf{R})$ over the asymptotic distribution function $f(\mathbf{R},\tau\to\infty) \sim f_0(\mathbf{R})$. The latter is arrived at by a stochastic propagation in imaginary time,

$$f(\mathbf{R}',\Delta\tau) = \int \tilde{G}_I(\mathbf{R}\to\mathbf{R}',\Delta\tau) f(\mathbf{R},0) d\mathbf{R}, \quad (6)$$

from an initial ensemble of multi-dimensional configuration points, or 'walkers':

$$\Psi(\mathbf{R},\tau=0) \cong \sum_i \delta(|\mathbf{R}|_i - |\mathbf{R}|). \quad (7)$$

$\tilde{G}_I(\mathbf{R})$ is the importance-sampled Green function [20,22], and $\Delta\tau$ the discrete imaginary time propagation step. The DMC approach employs a short-time expansion for the importance-sampled Green function $\tilde{G}_I(\mathbf{R})$ [24]. We use the Metropolis acceptance check for each attempted move such that for arbitrary timesteps the number density of walkers is given by Ψ_T^2, while their weights are a stochastic sample of the local value of Ψ/Ψ_T. This has been shown to result in large reductions of the timestep error [24].

The trial function is given by a generalized product for a bosonic cluster of N atoms containing an atomic impurity [16]. We employ pairwise radial functions to represent the correlations between all components of the cluster:

$$\Psi_T(\mathbf{R};\mathbf{p}) = \prod_{i<j}^{N} \psi_{ij}(R_{ij};\mathbf{p}) \prod_{i=1}^{N} \chi_i(R_i;\mathbf{p}'). \quad (8)$$

Here R_i is the distance of the ith He atom from the specific adatom, R_{ij} is the distance between helium atoms i and j, and $\mathbf{p}$, $\mathbf{p}'$ denote the sets of adjustable parameters controlling each of the two different pair functions ψ_{ij} and χ_i, respectively. For the He–He pair, we used the four-parameter function:

$$\psi_{ij}(R_{ij}) = \exp\left(-\frac{p_5}{R_{ij}^5} - \frac{p_2}{R_{ij}^2} - p_0 \ln R_{ij} - p_1 R_{ij}\right), \quad (9)$$

with size-dependent parameters p_k optimized for pure ^4He_N [24]. For the He–Ak function we employed the isotropic component of an analytic fit to the ground state wavefunction of He–Ak dimer. This isotropic function has the form

$$\chi_i(R_i) = \exp\left(-\frac{p_5'}{R_i^5} - p_1' R_i\right). \quad (10)$$

As the clusters grow in size, each trial function was modified in its parameters in order to follow the increased spatial extension of each of them. The actual parameter values can be obtained on request from the authors.

The ground state energy E_0 is obtained from averaging the local energy $E_L(\mathbf{R})$ over the importance-sampled distribution function $f(\mathbf{R})$ in the asymptotic regime

$$\langle E_L\rangle = \frac{\int E_L(\mathbf{R}) f(\mathbf{R},\tau) d\mathbf{R}}{\int f(\mathbf{R},\tau) d\mathbf{R}} \overset{\tau\to\infty}{\longrightarrow} \frac{\int \Phi_0(\mathbf{R})\mathcal{H}(\mathbf{R})\Psi_T(\mathbf{R}) d\mathbf{R}}{\int \Phi_0(\mathbf{R})\Psi_T(\mathbf{R}) d\mathbf{R}} \equiv E_0. \quad (11)$$

The Monte Carlo walk converts the integrals over $f(\mathbf{R})$ into simple averages over the ensemble of walkers $\{\mathbf{R}_i\}$ and their associated weights $\{w_i\}$ [22–26]:

$$\langle \mathcal{A}\rangle \approx \frac{\sum_i^M w_i A(\mathbf{R}_i)}{\sum_i^M w_i}. \quad (12)$$

The introduced bias for operators $\hat{A} \neq H$ is expected to be markedly reduced as the time propagation tends to infinity. Our present calculations have explicitly tested this point by successively extending the total number of time steps till convergence within the indicated error values.

The radial distribution of any atom-atom distance relative to the chosen reference frame is

$$P_{rad}(\mathbf{R}) = \frac{1}{n}\sum_i^n \left\langle \frac{\delta(|\mathbf{R}|_i - |\mathbf{R}|)}{\mathbf{R}^2}\right\rangle_{walk}, \quad (13)$$

where $n = 1$ for the Ak atoms and $n = m$ for any of the m ^{4}He atoms in the cluster.

The radial distribution function can be easily converted to the spherically averaged radial atomic density distribution $\rho(\mathbf{R})$

$$\rho(\mathbf{R}) = \frac{n}{4\pi} P_{rad}(\mathbf{R}), \quad (14)$$

with n being the number defined above.

One can further obtain with the same procedure the cosine distributions associated with θ, the latter representing any of the possible angles between the bonds among the three atoms θ_{ijk}, with the normalization condition

$$\int_{-1}^{1} P_{tot}(\cos\theta) d\cos\theta = 1. \quad (15)$$

From the above one can also extract the direct angular dependence, $P_{tot}(\theta)$, subject to the same condition

$$\int_0^{\pi} P_{tot}(\theta) d\theta = 1. \quad (16)$$

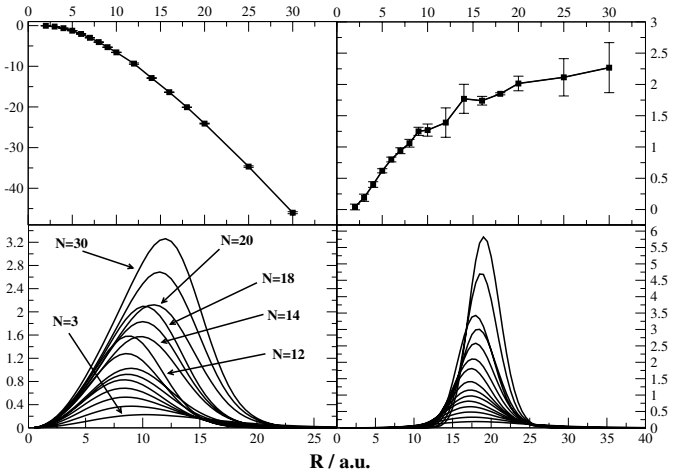

Fig. 2. Computed cluster properties with the lithium dopant, as a function of cluster size. Upper left panel: total binding energies (in cm^{-1} as a function of No. of He atoms). Upper right panel: single-He evaporative energies ($E_{tot}(N) - E_{tot}(N-1)$) as a function of cluster size. Lower left panel: radial density distributions (normalized to the No. of He atoms) showing helium distances from the geometric center of each cluster. Lower right panel: radial density distributions for the dopant lithium atom.

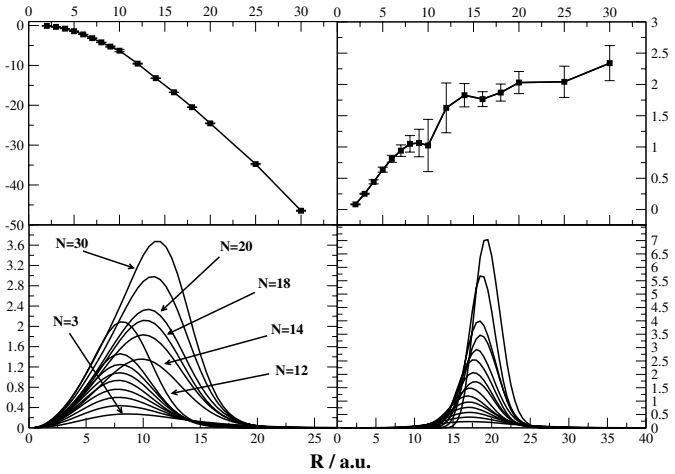

Fig. 3. Same computed quantities as those reported in Figure 2 but for the sodium-doped clusters.

We have also employed distance vectors which describe distributions from the geometric center of each cluster, R_{gc}, defined as

$$\mathbf{R}_{gc} = \frac{\sum_{i=1}^{N} \mathbf{R}_i + \mathbf{R}_{\rm Ak}}{N_{\rm He} + 1} \qquad (17)$$

which helps one to see more clearly the displacement of the dopant atom from the center of the cluster formed by the solvent atoms.

3 Results and discussion

The calculations were carried out using the trial functions discussed in the previous section. We employed each individual timestep $\delta\tau$ of about 25 atomic units and propagated out for a total of about 5000 steps, depending on the size of the cluster. The total number of blocks in the Monte Carlo propagation was around 2000 and each replica included about 2000 walkers. The total propagation in time was $25 \times 5000 \times 2000$ atomic time units. The final correlation length [24] was always close to 1.00 and never larger than 1.10. It was found that both cases of Li and Na as dopant required similar sets of numerical parameters.

The results of Figure 2 show, in the upper panel, the dependence of the total energies on cluster size for the case of the lithium dopant (left quadrant) while the general trend of single-particle (He) evaporative energies are shown by the right quadrant of the upper panel. The same set of results for sodium are shown by the two upper quadrants of Figure 3. All quantities carry a percentage error which remains, on average, below 1%.

Table 1. Computed energy values for the lithium-doped clusters as a function of the number of ^{4}He atoms.

N	E_{tot} (cm^{-1})	E^{He}_{evap} (cm^{-1})	E_{tot}/N	E^{Li}_{evap} (cm^{-1})
2	–0.041±0.005	0.041±0.005	–0.02	0.03
3	–0.23±0.01	0.19±0.01	–0.08	0.14
4	–0.63±0.01	0.40±0.02	–0.16	0.24
5	–1.25±0.02	0.62±0.03	–0.25	0.34
6	–2.05±0.02	0.80±0.04	–0.34	0.44
7	–2.99±0.03	0.94±0.05	–0.43	0.51
8	–4.05±0.03	1.06±0.06	–0.51	0.55
9	–5.30±0.03	1.25±0.06	–0.59	0.66
10	–6.57±0.06	1.27±0.09	–0.66	0.66
12	–9.35±0.17	1.39±0.23	–0.78	0.60
14	–12.89±0.06	1.77±0.23	–0.92	
16	–16.37±0.01	1.74±0.07	–1.02	
18	–20.07±0.01	1.85±0.02	–1.11	
20	–24.10±0.11	2.01±0.12	–1.20	
25	–34.67±0.19	2.11±0.30	–1.39	
30	–46.01±0.25	2.27±0.44	–1.53	

It is interesting to make the following comments in relation to the energetics shown by the present calculations: the total binding energies appear to smoothly increase for both dopants as cluster size increases. We therefore see no sign of shell formation but rather the uniform, liquid-like structures of pure helium clusters as discussed earlier by Lewerenz [27]. In other words, both sets of calculations indicate that the much weaker dopant interaction with the solvent atoms hardly contributes to keeping the cluster together and the latter essentially tends to behave as a pure cluster of helium atoms [27]. This point is also shown by the energies associated to evaporating one helium atom from the cluster: the values are very similar for both systems and resemble those of the pure helium clusters [27].

The fourth columns of Tables 1 and 2 also report the average energy change per ^{4}He atoms as the cluster

Table 2. Same computed energy indicators as those given by Table 1 but here for the case of the sodium-doped clusters.

N	$E_{tot}\,(\mathrm{cm}^{-1})$	$E_{evap}^{He}\,(\mathrm{cm}^{-1})$	E_{tot}/N	$E_{evap}^{Na}\,(\mathrm{cm}^{-1})$
2	–0.08±0.01	0.08±0.01	–0.04	0.07
3	–0.33±0.02	0.25±0.03	–0.11	0.25
4	–0.78±0.02	0.44±0.04	–0.19	0.39
5	–1.41±0.02	0.64±0.04	–0.28	0.51
6	–2.23±0.03	0.81±0.05	–0.37	0.61
7	–3.17±0.06	0.94±0.09	–0.45	0.69
8	–4.22±0.07	1.05±0.13	–0.53	0.72
9	–5.28±0.15	1.06±0.22	–0.59	0.64
10	–6.30±0.27	1.02±0.42	–0.63	0.40
12	–9.55±0.13	1.62±0.40	–0.80	0.81
14	–13.21±0.06	1.83±0.19	–0.94	
16	–16.74±0.06	1.76±0.12	–1.05	
18	–20.48±0.08	1.87±0.14	–1.14	
20	–24.54±0.10	2.03±0.18	–1.23	
25	–34.75±0.15	2.04±0.25	–1.39	
30	–46.45±0.13	2.34±0.28	–1.55	

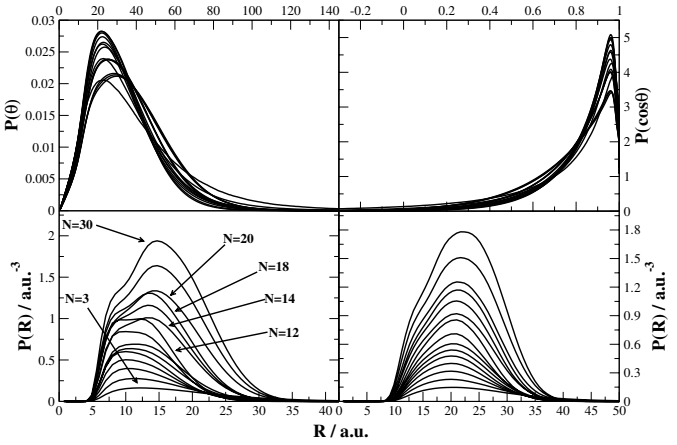

Fig. 4. Upper panels: computed distributions for the angle centered at the lithium atom and between any two helium adatoms ($\widehat{\mathrm{HeLiHe}}$). Left panel: probability distributions as a function of cluster size and over the angular range in degrees. Right panel: same distribution but given as a function of $\cos\theta$. Lower panels: computed atom-atom distance probability distributions as a function of cluster size. Left: distances between helium atoms; right: distances between lithium and helium atoms (radial distributions are all normalized to N_{He} atoms).

increases in size (E_{tot}/N) and one sees that such energy values tend to become essentially the same for both clusters as N increases. This means, in fact, that such changes become rapidly driven by the He–He interactions and therefore get to be independent of the dopant atom considered. Further comparison with estimates [28] of such a quantity in pure ^{4}He, provides in fact a value of about 1.6 cm^{-1} for pure clusters with N around 30, a value which is close to the present one reported by the 4th columns of the tables.

The binding energies of the dopant atoms to the cluster are also given in the last column of both tables, where comparison was possible only for the smaller clusters for which binding energies are available from previous calculations [27]: these calculations use the same He–He potential form [18]. One clearly sees there that the binding is much smaller than for the solvent atoms and reaches its largest value for $N = 10$ of about 0.91 K. Previous calculations that employed different pairwise potential report a value for clusters of the same size (see Fig. 5 of Ref. [14]) which is around 0.8 K and therefore in good agreement with our findings. They also suggest an asymptotic, bulk value of about 4.0 K: earlier density functional calculations [29] gave a value around 10 to 15 K for the binding energies of alkali atoms, but had neglected zero-point-energy contribution. We therefore see that the present results appear to agree better with the more accurate approach followed by [12].

If one now turns to the radial probability distributions computed for both doped clusters with respect to their geometric centers, see equation (17), we clearly see from both sets of lower panels reported by Figures 2 and 3 that the Ak dopants reside well outside the region where most of the helium atoms appear to be located. We also clearly see from both figures the strong spatial delocalization of all partner atoms and therefore the dominant role played by quantum effects on structural features. In spite of it, however, both lithium and sodium atoms distance themselves from the geometric center much more than the "solvent" helium atoms. This finding clearly confirms the results from entirely different (path-integral Monte Carlo) (PIMC) earlier calculations on the same systems [14], where it was also found that both Li and Na atoms should be considered as residing on the surface of the soft, liquid-like helium droplet. It is also interesting to note that in earlier work on the energetics of solvation [28] a dimensionless parameter λ was introduced, obtained from a simple model that included data like the surface tension, the cluster density and the features of the potential between the dopant and the helium atoms, taken as a simple pairwise potential [28]. Ancillotto et al. [29] therefore predicted that atoms with λ values of less than 1.9 would reside on the liquid surface, while those with larger λ values are expected to reside inside. Using the data [14] of bulk liquid helium and the energy parameters of the present pairwise potential, we find that $\lambda = 0.95$ for Li and $\lambda = 0.85$ for Na. Such values are therefore consistent with what has been found with present DMC calculations.

Other useful quantities regarding the cluster structures are provided by the probability distributions related of either the angular values between any three particles or the direct atom-atom distances between any two particles. Both sets of quantities are reported in Figure 4 for the lithium-doped calculations and in Figure 5 for the sodium-doped ones. The marked similarity of behaviour between the two systems is really striking.

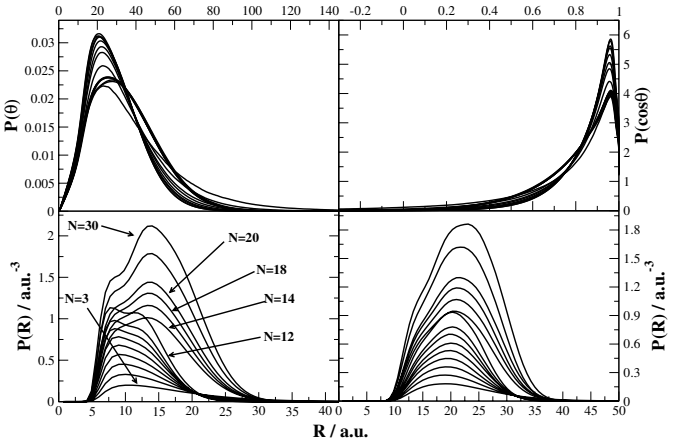

Fig. 5. Same computed quantities as those reported in Figure 4 but for the sodium-doped clusters.

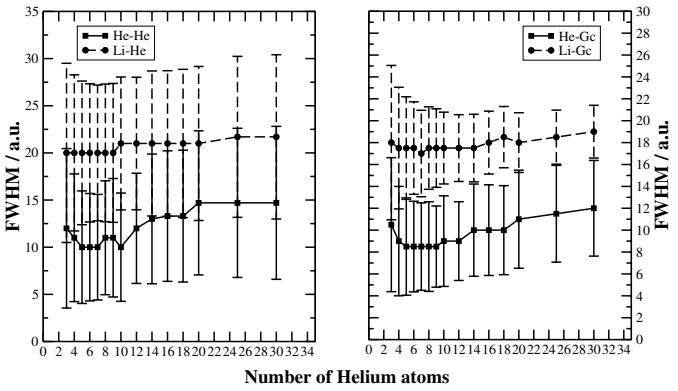

Fig. 6. Computed maxima of the radial probability distributions as a function of cluster size for the case of lithium dopants. The radial values pertain to atom-atom distances (left panel) or to distances from the geometric center (right panel). The bars for each maximum value represent a "delocalization index", i.e. the FWHM extracted from each probability distribution maxvalue.

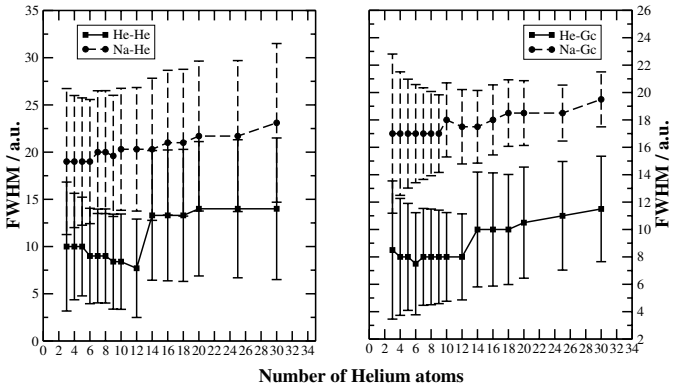

Fig. 7. Same set of data as those shown by Figure 6 but here referring to clusters with sodium dopants. See previous caption form meaning of symbols.

The angular distributions shown by those figures, in fact, confirm once again the very "floppy" structures of the clusters. They also show that, as the clusters grow bigger, the angles from the dopant atoms become increasingly smaller since their corresponding distances from any two ^{4}He atoms become larger while the average distance between those two atoms are reduced as the cluster becomes spatially larger as a whole but it creates a denser distribution (i.e. shorter He–He distances) of solvent atoms, a fact which thus explains the behaviour of the angular distributions from our calculations. In other words, both the Li and Na dopants show, from their angle distributions, that they monotonically move outside the clusters of helium atoms and therefore the corresponding probability distributions of all possible angles centred on the Ak atom and between any pair of He atoms move towards the smallest possible values; it is also interesting to note that the distributions pertaining to both dopants behave very similarly since the factor controlling such distributions is the migration of the alkali atom outside increasingly more compact and homogeneous helium clusters.

This type of behaviour is also visible from the data presented in the two sets of lower panels of Figures 4 and 5. We report there the probability distributions of the distances between pairs of ^{4}He atoms (left panels) and of the distances between the alkali atom and any of the helium atoms. One clearly sees that the He–He distributions are very similar in both cases and also closely resemble the distributions of pure helium clusters computed earlier on with very similar methods [27]. In other words, our calculations are creating in both situations essentially pure ^{4}He clusters that are chiefly stabilized by the dominant pairwise interactions between "solvent" atoms. On the other hand, the distances between either of the alkali atoms and any of the the ^{4}He adatoms in each cluster distribute themselves around maxima which are much greater and which describe a situation where the Li and Na impurity resides outside the cluster.

In Figures 6 and 7 we further show the plots of the maxima of the radial distributions, either using atom-atom distances (left panels) or atom distances from the geometric center (right panels).

In each of the figures, which list the distance maxima for the smaller clusters, we also report a sort of "delocalization bar" which indicates the value of the full distribution width at half maximum (FWHM) obtained from each radial distribution for which the maximum value is plotted in the figures. We therefore obtain a sort of "broad band" of radial delocalization for both the solvent atoms and the dopants: the picture we get is thus one of a "soft" liquid cluster over which floats the corresponding alkali atom. This is again in good accord with the predictions from previous calculations [14,28] and from experimental findings [4,11,15].

4 Present conclusions

In the present work we have carried out quantum Diffusion Monte Carlo calculations for a series of small clusters of bosonic helium that contain an alkali atom as a neutral dopant. We have considered the cases of lithium and sodium as alkaline impurities and have described the overall interaction according to equation (1), i.e. as a sum of pairwise interaction potentials that disregard as negligible the many-body effects originating from multiple interaction contributions. Such an approach has been the one most commonly employed for bosonic helium clusters interaction with neutral dopants (e.g. see Refs. [4,7,9]) and the results have usually been found in good accord with the experimental estimates [1].

The energetics of the calculations clearly show the marked dominance of the interactions between "solvent" atoms over the strength of the solvent-helium interactions, i.e. one sees that the total energies smoothly increase for small clusters in a fashion which is similar for both dopants and strongly reminiscent of the behaviour for pure ^{4}He clusters [27]. The binding energies of helium atoms to the clusters also turn out, as expected, to be larger than those of the dopant's atoms and rapidly become independent of the alkali atom present in the clusters. Finally, our estimate of the alkali atom's binding energy to the largest cluster for which a comparison was possible ($N = 10$) turn out to be very close to that given by earlier, accurate quantum calculations [14] which used an entirely different approach and interaction potentials.

The analysis of the radial probability densities obtained from the present calculations further allowed us to draw the following conclusions:

1. the distributions of the distances of both the dopant and the solvent adatoms from the geometric centers of the clusters, as defined by equation (17), clearly indicate that the alkali atoms reside mainly outside the cluster, the latter being mostly formed by the bosonic helium atoms;
2. our calculations show that the He–He distances rapidly acquire distribution shapes and values which are very close to the pure helium clusters while the alkali atoms show radial distributions that are much larger and tend to increase with the size of the cluster. The analysis of the corresponding angular distributions, for the angles centered at the alkali atoms within the clusters, also indicates that those distributions become increasingly narrower as N increases and further show a marked maximum around $\theta = 20$. This feature suggests, therefore, that the dopant atom is moving further outside the cluster as N increases and its distances from any pair of helium "solvent" atoms are in the main much larger than the corresponding distances between any of two helium atoms among themselves;
3. by considering the dependence of the maximum values of the radial distributions on the N values (see Figs. 6 and 7) for both the alkali and the helium atoms, we were able to show that the dopants are indeed "floating" on the ^{4}He clusters and invariably appear to remain outside the small aggregates we have analysed in the present study.

It is also interesting to note that recent DMC calculations[30] on the energetics of the $Li_2(^1\Sigma_g^+)$ as a dopant in small helium clusters indicate their binding energies to be even smaller than those reported for the monomer in Table 1. Thus, it is reasonable to suggest that the lack of observation of its excitation spectra [15] could be due to its fast evaporation on cluster break up. On the other hand, our recent calculations on the $Li_2(^3\Sigma_u^+)$ indicate stronger binding [31], which would make its stability upon excitation more likely to occur.

In conclusion, we feel that the present calculations has indeed confirmed within a quantum approach the suggestions coming from the analysis of the experiments [4,5,11] and also the finding from earlier calculations [14,29] which employed an entirely different approach.

The financial support of the EU Network on "Cold Molecules" (HPRN-CT-2002-00290), of the University of Rome "La Sapienza" Research Committee and the INFM research Committee are gratefully acknowledged. We are also grateful to the CASPUR Supercomputing Consortium for having provided help and advice on the computational aspects of this study.

References

1. J.P. Toennies, A.F. Vilesov, Angew. Chem. Int. Ed. **43**, 2622 (2004)
2. S. Grebenev, J.P. Toennies, A.F. Vilesov, Science **279**, 2083 (1998)
3. J.P. Toennies, A.F. Vilesov, Ann. Rev. Phys. Chem. **49**, 1 (1998)
4. F. Stienkemeier, A.F. Vilesov, J. Chem. Phys. **115**, 10119 (2001)
5. F. Brhül, R.A. Trasca, W.E. Ernst, J. Chem. Phys. **115**, 10220 (2001)
6. D. López-Durán, M.P. de Lara-Castells, G. Delgado Barrio, P. Villareal, C. Di Paola, F.A. Gianturco, J. Jellinex, J. Chem. Phys. **121**, 2975 (2004)
7. E.g. see: F. Sebastianelli, E. Bodo, I. Baccarelli, C. Di Paola, F.A. Gianturco, M. Yurtsever, J. Mater. Sci. (2005, in press)
8. A. Nakayama, K. Yamashita, J. Chem. Phys. **112**, 10966 (2000)
9. F. Sebastianelli, C. Di Paola, I. Baccarelli, F.A. Gianturco, J. Chem. Phys. **119**, 5570 (2003)
10. J. Jortner, N.R. Kestner, S.A. Rice, M.M. Cohen, J. Chem. Phys. **43**, 2614 (1965)
11. F. Stienkemeier, J. Higgins, W.E. Ernst, G. Scoles, Z. Phys. B **98**, 413 (1995)
12. F. Stienkemeier, O. Bünermann, R. Mayol, F. Ancillotto, M. Barranco, M. Pi, Phys. Rev. B **70**, 214509 (2004)
13. O. Bünermann, M. Mudrich, M. Weidemüller, J. Chem. Phys. **12**, 8880 (2004)
14. A. Nakayama, K. Yamashita, J. Chem. Phys. **114**, 780 (2001)
15. F. Stienkemeier, J. Higgins, C. Callegari, S.I. Kanorsky, W.E. Ernst, G. Scoles, Z. Phys. D **38**, 253 (1996)

16. C. Di Paola, F.A. Gianturco, F. Paesani, G. Delgado-Barrio, S. Miret-Artés, P. Villarreal, I. Baccarelli, T. Gozález-Lezana, J. Phys. B **35**, 2643 (2002)
17. U. Kleinekathöfer, K.T. Tang, J.P. Toennies, C.L. Yiu, J. Chem. Phys. **107**, 9502 (1997)
18. K.T. Tang, J.P. Toennies, C.L. Yiu, Phys. Rev. Lett. **74**, 4571 (1995)
19. U. Kleinekathöfer, K.T. Tang, J.P. Toennies, C.L. Yiu, Chem. Phys. Lett. **249**, 257 (1996)
20. B.L. Hammond, W.A. Lester Jr, P.J. Reynolds, *Montecarlo Methods in Ab Initio Quantum Chemistry* (World Scientific, Singapore 1994)
21. D.M. Ceperley, B. Alder, Science **231**, 555 (1994)
22. M.A. Suhm, R.O. Watts, Phys. Rev. **204**, 293 (1991)
23. J. Anderson, J. Chem. Phys. **63**, 1499 (1975)
24. M. Lewerenz, J. Chem. Phys. **104**, 1028 (1996)
25. D. Blume, M. Lewerenz, F. Huisken, M. Kaloudis, J. Chem. Phys. **105**, 8666 (1996)
26. P.J. Reynolds, D.M. Ceperley, B. Alder, W.A. Lester Jr, J. Chem. Phys. **77**, 5593 (1982)
27. M. Lewerenz, J. Chem. Phys. **106**, 4596 (1997)
28. V.R. Pandharipande, J. G. Zabolitzky, S.C. Pieper, R.B. Wiringa, U. Helmbrecht, Phys. Rev. Lett. **50**, 1676 (1983)
29. F. Ancillotto, P.B. Lerner, M.W. Cole, J. Low Temp. Phys. **101**, 1123 (1995)
30. E. Bodo, F.A. Gianturco, F. Sebastianelli, E. Yurtsever, M. Yurtsever, J. Chem. Phys. **120**, 9160 (2004)
31. E. Bodo, F.A. Gianturco, E. Yurtsever, M. Yurtsever, umpublished results